Experimental study on geosynthetic-reinforced sand fill over marine clay with or without deep cement mixed soil columns under different loadings

Pei-Chen Wu, Jian-Hua Yin [*], Wei-Qiang Feng, Wen-Bo Chen

Department of Civil and Environmental Engineering, The Hong Kong Polytechnic University, Hong Kong, China

Abstract

Geosynthetics and deep cement mixed (DCM) soil columns have been widely used to improve soft soil grounds in many countries and regions. This paper presents an experimental study on a geosynthetic-reinforced sand fill over marine clay with or without DCM columns under different loadings. Two tests were conducted on the sand fill reinforced with fixed-end and free-end geosynthetics over marine clay under three-stage local loading to investigate the effects of the boundary conditions of geosynthetic reinforcement on reducing settlements. It is observed that the fixed-end geosynthetic sheet is more effective in reducing settlements than the free-end condition under identical local loading. Another test was conducted on the fixed-end geosynthetic-reinforced sand fill over the marine clay improved by DCM columns under single-stage uniform loading. The vertical stresses on the marine clay and on the DCM columns, as well as the tensile strains of the geosynthetic sheet in the overlying sand fill, were measured. The results revealed that the stress concentration ratio increases with an increase in consolidation settlements, and the maximum tensile strain of the geosynthetic sheet occurs near the edge rather than at the center of the top surface of the DCM columns.

1 Introduction

Geosynthetics and deep cement mixed (DCM) soil columns have been widely used to improve soft soil grounds for constructions of, for example, highway embankments, seawalls, and building foundations, and also for covering excavated and backfilled trenches. Geosynthetics, such as geotextiles and geogrids, have been widely used for many applications in geotechnical engineering. Geosynthetics are mainly used for reinforcement, filtration, separation, drainage, protection, and as fluid barriers (Shukla & Yin, 2006). The protection function of geotextiles and the ero-

sion behavior of the geotextile revetment under bi-directional cyclic flow were examined by Ho (2007). A physical model test was conducted by Feng, Li, Yin, Chen, and Liu (2019) to investigate the separating effect of geotextile on the interface between Hong Kong marine clay and a sand fill. The effects of the geosynthetic reinforcement on controlling settlement, reducing the required height of granular fill, and enhancing the bearing capacity of soft clay subgrade were studied in both small-scale and large-scale physical model tests (Biswas, Asfaque Ansari, Dash, & Krishna, 2015; Demir, Laman, Yildiz, & Ornek, 2013; El Sawwaf, 2007; Roy & Deb, 2017). However, most of the above studies did not consider the boundary condition influences of the geosynthetic sheet. For geotextile, Espinoza and Bray (1995) indicated that the membrane

---

* Corresponding author.

E-mail addresses: peichen.wu@connect.polyu.hk (P.-C. Wu), cejhyin@polyu.edu.hk (J.-H. Yin), sam.feng@polyu.edu.hk (W.-Q. Feng).

support effect of geotextiles can be developed through not only shear stresses but normal stresses when fixing the edges of geotextiles. Liu, Kong, Li, Ding, and Gu (2008) found that the effect of a free-end geogrid on reducing differential settlements of the soft foundation of an expressway was not significant. Later, a new ground improvement technique involving fixed-geosynthetic reinforcement and pile supports was proposed by Zhang, Zheng, Chen, and Yin (2013). It was revealed that the fixed-geosynthetic reinforcement can reduce both total and differential settlements sufficiently. However, to the best of the authors' knowledge, few studies have directly investigated the influence of boundary conditions on settlement behavior.

The deep mixing technique, which was originally developed in Sweden and Japan, is used to stabilize and modify soil by adding binders, such as lime, cement, or other additives (Hausmann, 1990; Kitazume & Terashi, 2013). Portland cement has been widely utilized to treat marine clay. The mechanical and chemical properties of cement mixed clay have been investigated for decades (Chew, Kamruzzaman, & Lee, 2004; Kamruzzaman, Chew, & Lee, 2006, 2009; Yin & Lai, 1998). Yin and Fang (2006) studied the consolidation behavior of a composite foundation of soft marine clay improved by a deep cement mixed (DCM) soil column by using a small-scale model test. Afterwards, Yin and Fang (2010) investigated the behavior of DCM improved soft clay ground under a rigid footing and observed wedge-shaped block failure. In another study, the bearing capacity and failure mechanism of soft soil improved by DCM columns under both rigid and flexible footings were examined by Rashid, Black, Kueh, and Noor (2015). Although the arching effect in column- or pile-supported embankments has been studied by many scholars (Abusharar, Zheng, Chen, & Yin, 2009; Chen, Chen, Han, & Xu, 2008; Lai, Zheng, Zhang, & Cui, 2018; Russell & Pierpoint, 1997; Zhuang, Wang, & Liu, 2014), the investigation of the loading distribution between soils and reinforcements when considering the fixed-end condition of a geosynthetic sheet can still yield useful results.

In this paper, an experimental study including three physical model tests is presented. The objectives of this experimental study are as follows: (a) to investigate the effect of the boundary conditions of a geosynthetic sheet on reducing the settlements of a sand fill over marine clay, and (b) to monitor the vertical stresses on the marine clay improved by DCM columns and the tensile strain of the geosynthetic sheet in the overlying sand fill. For the first objective, two physical model tests were conducted on a sand fill reinforced by fixed-end and free-end geosynthetics over marine clay under three-stage loading. For the second objective, one physical model test was performed for the sand fill reinforced by a fixed-end geosynthetic sheet over marine clay improved by DCM columns under single-stage uniform loading.

2 Experiment

The details of the three physical model tests (Test 1, Test 2, and Test 3) involved in this experimental study are listed in Table 1. Each physical model was 1 000 mm long, 300 mm wide, and 700 mm tall. Figure 1 shows that the physical model comprises two layers of soils: a subgrade marine clay and an overlying reinforced sand layer. Test 1 and Test 2 were conducted to investigate the effect of different boundary conditions of geosynthetic reinforcement (free-end and fixed-end) on settlement under three-stage local loading. The duration of each stage of loading was three days. In Test 3, which involved DCM columns, uniform loading was applied. The vertical stresses on DCM columns and surrounding clay, as well as the tensile strains of the geosynthetic sheet, were monitored during the test. Four fiber Bragg grating (FBG) sensors were attached to the geosynthetic sheet in Test 3 by using an epoxy resin. The locations of the installed FBG sensors were 0 mm (mid-span, over the surrounding clay), 180 mm (near the edge of the DCM column), 250 mm (over the center of the DCM column), and 400 mm (over the surrounding clay) from the center of the geosynthetic sheet along the length direction of the physical model, as shown in Fig. 1.

Traditional earth pressure transducers, which work based on strain gauges, were used by Yin and Fang (2006) to monitor vertical stresses. Similarly, in Test 3, two earth pressure transducers based on the FBG sensing technique (FBG-EPCs) were utilized to monitor the total vertical stresses on the DCM column and surrounding clay, respectively. The FBG-EPC transducer and FBG sensor are shown in Fig. 2. The earth pressure transducers comprise a stainless-steel cell and an FBG sensor. The FBG sensor was attached to the inside surface of a flexible plate on top of the stainless-steel cell. When the FBG-EPC is installed in soils, the outer surface of the plate will deform under pressure. The deformation of the plate is then transferred to the FBG sensors and changes the wavelength of the sensors, which can be recorded by an interrogator. By calibrating the transducers using water pressure, the relationship between the applied pressure and the wavelength of the FBG sensors can be obtained. A strongly linear relationship is observed between the calibrated pressure and the wavelength change of the FBG -EPCs for both the measured stress over the DCM column and that over the surrounding soft clay, as shown in Fig. 3. The sensitivity of the FBG-EPCs is 0.001 5 nm/kPa.

2.1 Materials

The marine clay used in this study was originally taken from a coastal area near Lantau Island in Hong Kong and reconstituted in a laboratory. The basic properties of the marine clay are as follows: a specific gravity of 2.63, a liquid limit of 57.1%, a plastic limit of 25.2%, and a plasticity index of 31.9 %. The mechanical parameters of the marine

Table 1
Test information.

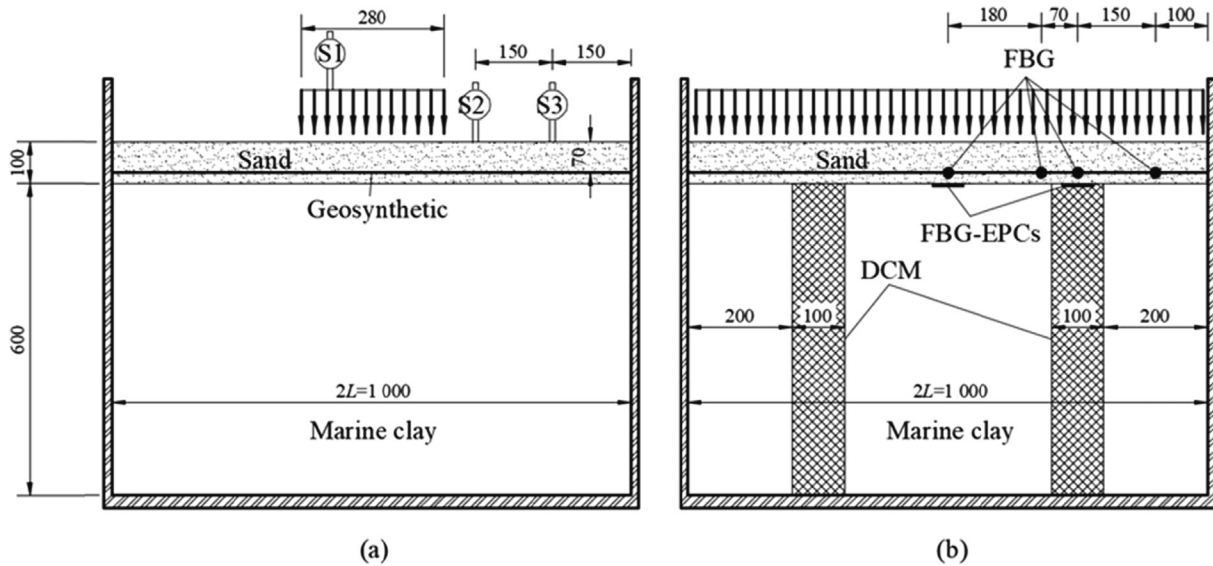| Test No.	Loading	Geosynthetic	DCM columns	Time (d)
Test 1	Local loadings: 5 kPa, 10 kPa, 15 kPa	Free ends	—	9
Test 2	Local loadings: 5 kPa, 10 kPa, 15 kPa	Fixed ends	—	9
Test 3	Uniform loading: 15 kPa	Fixed ends	2	3

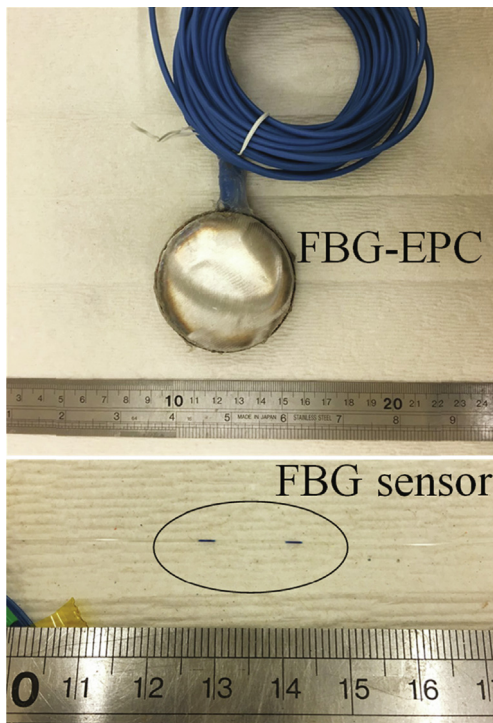Fig. 1. Schematic diagram of tests: (a) Test 1 and Test 2, and (b) Test 3 (unit in mm).

Fig. 2. FBG-EPC transducer and FBG sensor.

the creep coefficient ψ/V. The definitions of those parameters can be found in Yin and Graham (1994). The basic properties of the sand are as follows: a specific gravity of 2.65, a minimum dry density of 1.485 g/cm^3, a maximum dry density of 1.665 g/cm^3, an optimum moisture content of 16.4%, and a unit weight of 18.3 kN/m^3 (80% relative density with a moisture content of 12.8%). The consolidated drained strength parameters of the sand are as follows: a cohesion c' of 2.48 kPa and a friction angle φ' of 37.4°. The particle size distributions of the marine clay and sand are shown in Fig. 4. One type of extruded geogrid with an aperture of 2 cm × 2 cm and a tensile modulus of 140 kN/m was selected as the geosynthetic reinforcement.

2.2 Test preparations and procedures

The marine clay was mixed and reconstituted with water by a miniature motorized mixer (Yin & Fang, 2010). The subgrade was prepared using the reconstituted marine clay that was pre-consolidated under 10 kPa with the help of prefabricated vertical drain (PVD) bands to hasten the consolidation process. After finishing the pre-consolidation stage, the sand fill was laid and gently compacted to the desired thickness. In Test 1, a layer of geosynthetic sheet was simply laid in the sand fill, as shown in Fig. 1, while in Test 2, clamps and bolts were used to anchor the geosynthetic sheet to the walls of the steel tank. Later, the top layer of the sand was filled and compacted. Three dial

clay obtained from an oedometer test were as follows: 0.067 for the slope of the reference time line λ/V, 0.017 5 for the slope of the instant time line κ/V, and 0.002 6 for

(a)

$y = 0.001\,5x + 1\,545.90$
$R^2 = 0.999\,3$

(b)

$y = 0.001\,5x + 1\,577.90$
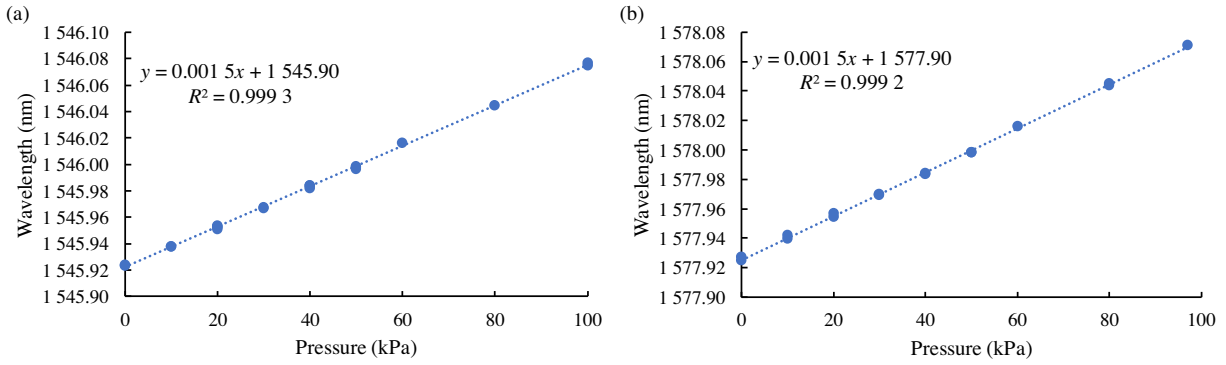$R^2 = 0.999\,2$

Fig. 3. Calibration of FBG-EPCs: (a) FBG-EPC over DCM column; (b) FBG-EPC over surrounding clay.
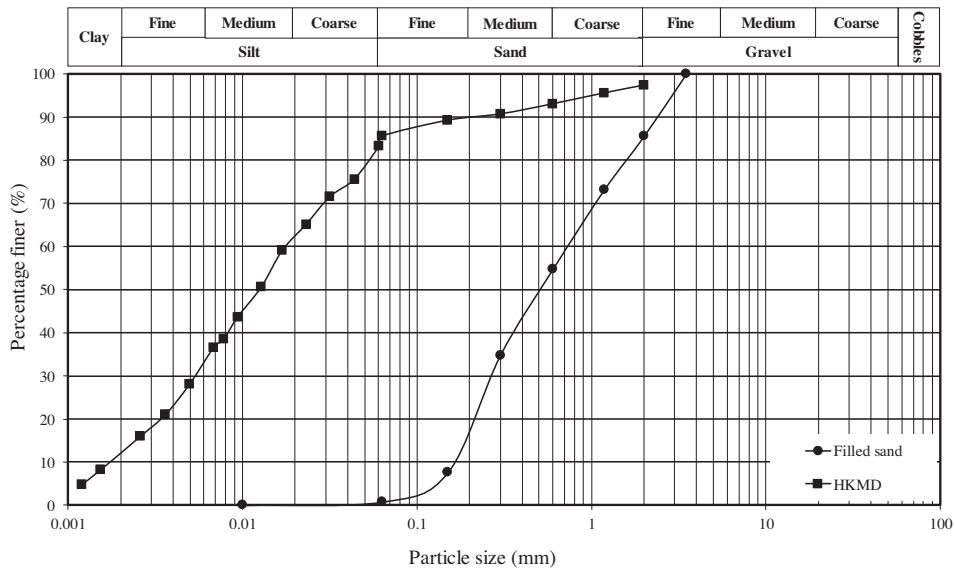

Fig. 4. Particle size distributions of marine clay and sand.

gauges were installed on the sand fill to measure the surface settlements during each test. Three stages of local loadings, i.e., 5 kPa, 10 kPa, and 15 kPa, were applied in the physical model with a total loading duration of 9 d in both free-end (Test 1) and fixed-end (Test 2) cases. Each stage of loading was applied for 3 days.

In Test 3, after finishing the pre-consolidation stage, holes were drilled at pre-determined locations in the marine subgrade to install DCM columns. It should be noted that the DCM columns were made by mixing the excavated clay with cement at a cement–soil ratio (in dry mass) of 20%. Two DCM columns were mixed and cast in an identical manner to keep the properties consistent. Furthermore, they were cured individually to ensure their quality and then installed into the prepared holes in the subgrade. Subsequently, the subgrade was overlaid with the reinforced sand fill according to the procedure used in Test 2. Before installing the geosynthetic sheet, FBG sensors were attached to desired locations on the geosynthetic sheet by epoxy glue. A uniform loading of 15 kPa was applied to the entire sand fill and maintained for 3 days.

3 Results and discussions

3.1 Results of Test 1 and Test 2

The surface settlements were measured by dial gauges (S1, S2, and S3) at different locations, as shown in Fig. 1. In Figs. 5 and 6, the hollow circles denote the settlements measured in Test 1 corresponding to the free-end condition, while the crosses are the measured settlements in Test 2 corresponding to the fixed-end condition.

Instant settlements under the loading region were observed at 0 d, 3 d, and 6 d, when vertical stresses of 5 kPa, 10 kPa, and 15 kPa were applied, respectively. Every instant settlement was followed by a consolidation settlement that lasted 3 d. Figure 5 shows that the slopes of the curves of the settlements measured by dial gauges S1 and S2 in the first two stages are less than those in stage 3. It might be attributed to the fact that the subgrade under the loading region in stage 1 and stage 2 was at a state of slightly over-consolidation while the subgrade in stage 3 was at the normally consolidated state.
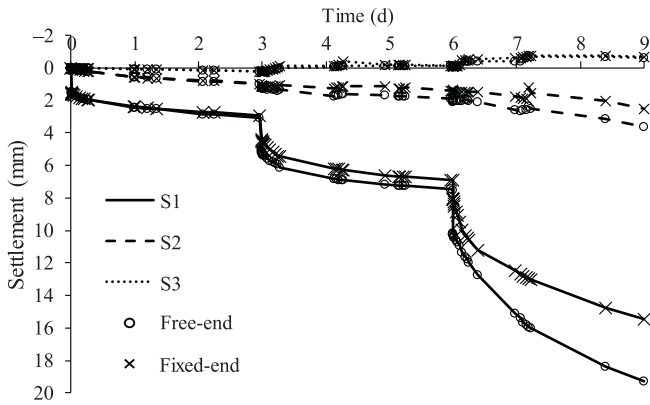
Fig. 5. Measured settlements of Test 1 and Test 2 at different locations.

There was no significant difference between the settlement observed in cases of the free-end condition and that of the fixed-end condition under the loading of 5 kPa. However, after loadings of 10 kPa and 15 kPa were applied, the measured settlements in the case of the fixed-end condition were less than those in the free-end condition. This means that the fixed-end geosynthetic sheet is more effective in reducing settlements than the free-end geosynthetic sheet. Meanwhile, there were slight heaves in both free-end and fixed-end conditions at stage 2 and stage 3.

The profile curves of the settlements after 3 d, 6 d, and 9 d for both fixed-end and free-end conditions are plotted in Fig. 6. The horizontal axis is the distance from the center of the reinforced sand fill. Although apparent differential settlements are observed near the loading area for both cases, fewer differential settlements were observed in the case of the fixed-end condition. Compared with the free-end condition, the fixed-end condition results in differential settlement decreases of 4.15% after 3 d under 5 kPa, 7.31% after 6 d under 10 kPa, and 18.85% after 9 d under 15 kPa. The maximum settlements in the fixed-end condition decrease 5.08% under 5 kPa, 7.63% under 10 kPa, and 19.9% under 15 kPa compared with the free-end condition. It is observed that the fixed-end geosynthetic sheet

controls differential settlements and reduces maximum settlements. This effect increases as the applied load increases. However, the long-term behavior of the fixed-end geosynthetic sheet should be further investigated while considering the creep of marine clay.

3.2 Results of Test 3

3.2.1 Vertical stress and stress concentration ratio

Two FBG-EPCs were installed to monitor the vertical stresses on a DCM column and the surrounding clay, as shown in Fig. 1(b). Figure 7 shows the vertical stresses on the column and the surrounding clay with time. There is an increasing trend in the stress on the DCM column, while the stress on the surrounding clay is nearly stable. Low, Tang, and Choa (1994) proposed the concept of a stress-reduction ratio, which can be defined as the ratio of the loading on the soft soil to the loading of the overlying granular material, to reflect the arching effect. If the stress-reduction ratio equals 1.0, this indicates no arching, which means the loading on the columns equals the loading on the surrounding clay. In Test 3, the overlying granular material was subjected to a uniform loading of 15 kPa. The equivalent height of the sand fill H_e ($H_e = h_c + h$, where h_c is converted height, h is original height of the sand
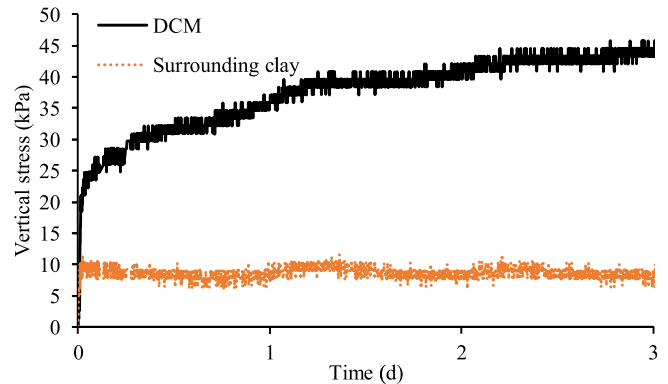

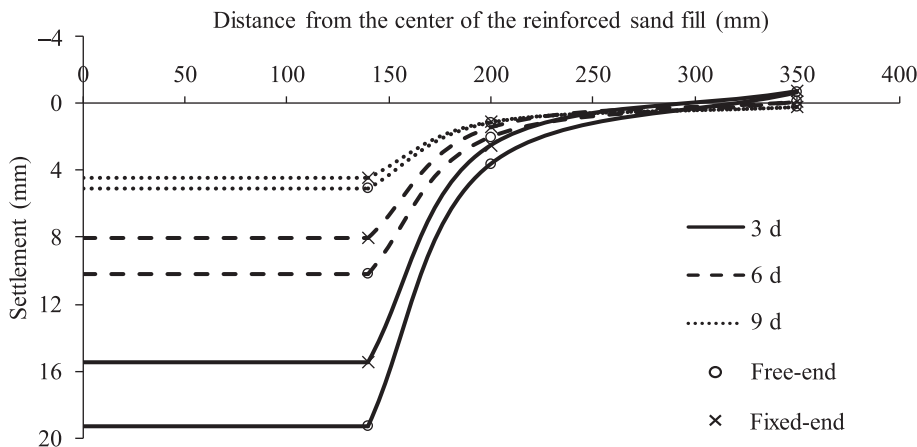Fig. 7. Measured vertical stresses on surrounding clay and DCM column with time from Test 3.

Fig. 6. Settlement profiles at 3 d, 6 d, and 9 d for Test 1 and Test 2.

fill) is calculated according to vertical stress equilibrium, as illustrated in Fig. 8.

Ariyarathne and Liyanapathirana (2015) proposed an equation based on a modification of BS 8006 (van Eekelen, Bezuijen, & Van Tol, 2011) to calculate the stress-reduction ratio ξ for the situation of full arching, as shown in Eq. (1)

$$\xi = \frac{1.4}{H(s+a)}\left[s^2 - a^2\left(\frac{P_c}{\gamma H}\right)\right], \text{ for } H > 0.7(s-a), \qquad (1)$$

where s is the spacing between adjacent columns, a is the diameter of the columns, H is the height of the sand fill (equivalent height H_e is used in this study), and P_c is the vertical stress on the columns. For the end-bearing columns, BS 8006 (2010) recommends the following equation:

$$P_c/\gamma H = [(1.95H/a - 0.18)a/H]^2. \qquad (2)$$

After converting the vertical loading into an equivalent sand fill, H_e is 0.92 m, which meets the condition for full arching. According to Eq. (1), the stress-reduction ratio ξ is 0.54, while the stress-reduction ratio ξ calculated by the measured vertical stresses is 0.59. It seems that Eq. (1) slightly overestimates the stress-reduction ratio. This might be due to (a) using an equivalent height of sand fill obtained by directly converting the applied loading to a height value and/or (b) installing a fixed-end geosynthetic sheet. For the first reason, directly converting the applied loading to an equivalent height of sand fill by using vertical stress equilibrium (the same vertical stresses before and after converting) inevitably overestimates the soil arching effect, because the shear stress that assists in loading transfer in the equivalent sand fill does not actually exist. Therefore, the overestimated arching effect is reflected by the lower value of the stress-reduction ratio calculated by Eq. (1).

The second reason can be illustrated by calculating the value of $P_c/\gamma H$. According to the measured vertical stress on the DCM columns, the value of $P_c/\gamma H$ is approximately 2.673, while the value of $P_c/\gamma H$ calculated using Eq. (2) is 3.726. Because the fixed-end geosynthetic sheet provides resistance forces in an upward direction, the vertical stresses on the columns and marine clay decrease. Therefore,

Eq. (2) recommended by BS 8006 (2010) yields an overestimated result.

The resultant force can be defined and calculated by Eq. (3)

$$F = A_{clay}\sigma_{clay} + A_{DCM}\sigma_{DCM}, \qquad (3)$$

where A_{clay} is the area of the surrounding clay, A_{DCM} is the area of the DCM column, σ_{clay} is the stress on the surrounding clay, and σ_{DCM} is the stress on the DCM column, which equals P_c. In the above equation, it is assumed that the vertical stress measured in the middle of the clay is identical to the stresses in other areas of the surrounding clay. It is also assumed that the stresses on the two DCM column are identical. Figure 9 shows the resultant force (marked as "Measured"), which is calculated by Eq. (3) using measured stresses versus time and the applied resultant force, which is calculated using the known applied uniform pressure multiplied by the total area, versus time. It is observed that the applied resultant force is almost 1.5 times the measured resultant force. This is mainly because the fixed-end geosynthetic sheet has provided resistance forces in the upward direction, thereby reducing the measured resultant force.

In the next step, the stress concentration ratio is defined as $n = \sigma_{DCM}/\sigma_{clay}$ and variation in stress concentration ratio versus time is plotted in Fig. 10. It is clearly shown that the values of stress concentration ratio increase with the consolidation settlement of soils. The vertical stress on the surrounding marine clay is gradually transferred to the DCM columns when the excess pore water pressure dissipates and the ground settlement is monitored. This is because the stiffness of the DCM columns is different from that of the surrounding marine clay, and the stress would adjust along the consolidation settlement to minimize the differential settlement on the surface. This phenomenon was also found and presented by Yin and Fang (2006). As the area replacement ratio of the DCM column-treated marine clay in their physical model was 2.77%, which is less than the area replacement ratio in this study, the stress concentration ratio measured by Yin and Fang (2006) is larger than that in this study because smaller area replacement ratios result in larger stress concentration ratios (Sexton, Sivakumar, & McCabe, 2017).
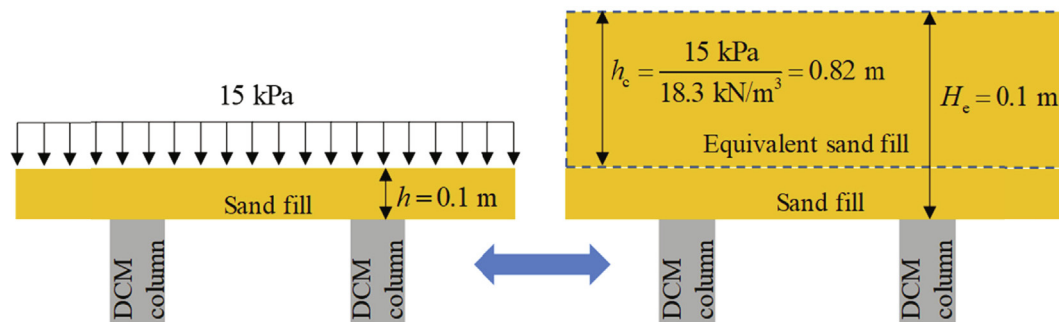

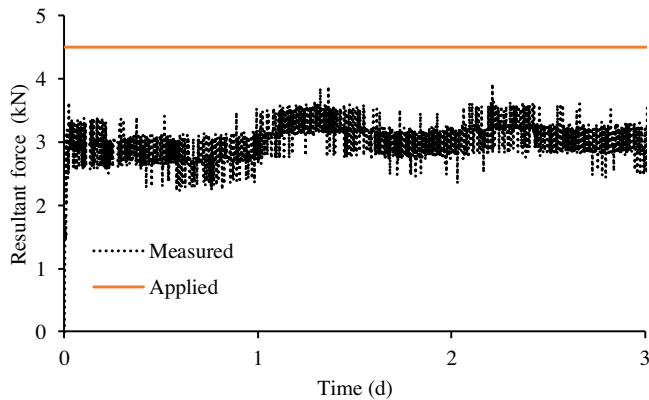Fig. 8. Equivalent height of the sand fill.

Fig. 9. Measured resultant force and applied resultant force with time from Test 3.
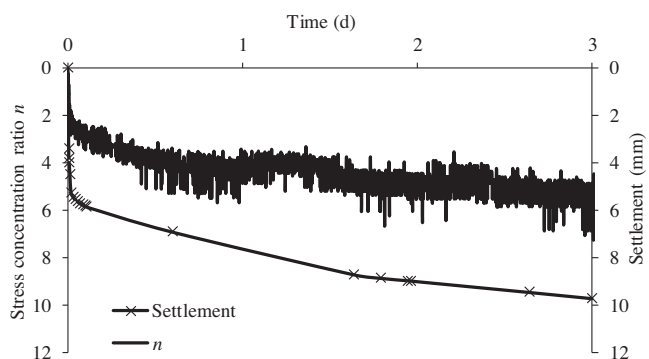

Fig. 10. Measured stress concentration ratio and settlement with time from Test 3.

3.2.2 Tensile strain

The tensile strains in the geosynthetic sheet were measured by FBG sensors. These sensors were located at 0 mm (mid-span over the surrounding clay), 180 mm (near the edge of the DCM column), 250 mm (over the center of the DCM column), 400 mm (over the surrounding clay) along the length direction from the center of the geosynthetic sheet. The distributions of the tensile strain in the geosynthetic sheet reinforcement after 1 d, 2 d, and 3 d are shown in Fig. 11.

It is observed that the tensile strain of the geosynthetic sheet is mainly monitored near the edge of DCM columns,
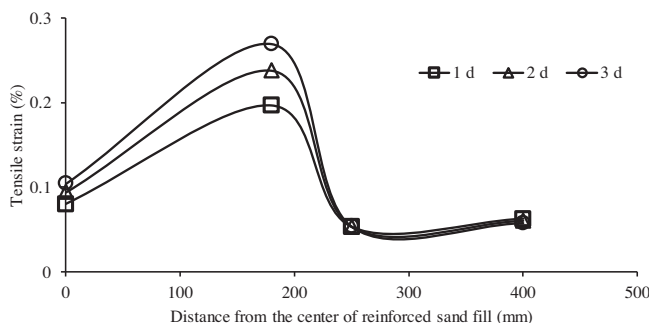

Fig. 11. Distribution of tensile strains of geosynthetic reinforcement after 1 d, 2 d, and 3 d for Test 3.

and the tensile strain changes little at the top of the column. Given the stiffness difference between the DCM column and the marine clay, the relative deformation mainly occurs at the edge of the DCM column, and this relative deformation results in the tensile deformation of the geosynthetic sheet. Thus, in a real experimental study, the geosynthetic sheet effect is not displayed evenly, except at a certain location. The tensile strain of the geosynthetic sheet on the mid-span (0 mm) shows a slight increase with time, while the strain of the geosynthetic sheet over the surrounding clay at the location of 400 mm to the center shows almost no change. Fei and Liu (2009) observed a similar phenomenon by using a finite element simulation.

4 Findings

In this work, three experimental studies were conducted to investigate the performances of a geosynthetic sheet reinforced sand fill over marine clay with or without DCM columns. Test 1 and Test 2 compared the settlements of the geosynthetic sheet reinforced sand fill over marine clay under three-stage local loading to examine the effects of different boundary conditions of the geosynthetic sheet. In Test 3, the stress concentration ratio and the tensile strains of the fix-end geosynthetic sheet were monitored for the marine clay reinforced with the DCM columns. Based on these investigations, the following findings are obtained:

(a) In Test 1 and Test 2, the settlement can be reduced effectively by using fixed geosynthetic reinforcement as opposed to free-end geosynthetic reinforcement. It is noted that slight heaves instead of settlements were observed near the edge of the reinforced sand fill for both free-end and fixed-end conditions.

(b) In Test 3, where a fixed-geosynthetic-reinforced sand fill over marine clay improved by DCM columns was subjected to uniform loading, the vertical stress on the DCM column was larger than the stress on the surrounding soil owing to the arching with a stress-reduction ratio of 0.59. Moreover, the stress concentration ratio increases with increasing consolidation settlement.

(c) The resultant force of the applied uniform loading is approximately 1.5 times the calculated resultant force based on the measured stresses. This is mainly because the fixed-end geosynthetic sheet provides resistance forces in an upward direction, thus reducing the measured resultant force.

(d) The maximum tensile strain of the fixed-end geosynthetic reinforcement was observed near the edge of the top of DCM columns rather than at the center.

Acknowledgements

Conflict of interest

There is no conflict of interest.

References

Abusharar, S. W., Zheng, J. J., Chen, B. G., & Yin, J. H. (2009). A simplified method for analysis of a piled embankment reinforced with geosynthetics. *Geotextiles and Geomembranes, 27*(1), 39–52.

Ariyarathne, P., & Liyanapathirana, D. S. (2015). Review of existing design methods for geosynthetic-reinforced pile-supported embankments. *Soils and Foundations, 55*(1), 17–34.

Biswas, A., Asfaque Ansari, M., Dash, S. K., & Krishna, A. M. (2015). Behavior of geogrid reinforced foundation systems supported on clay subgrades of different strengths. *International Journal of Geosynthetics and Ground Engineering, 1*(3), 20.

BS 8006 (2010). *Code of practice for strengthened/reinforced soils and other fills.* British Standard Institution.

Chen, R. P., Chen, Y. M., Han, J., & Xu, Z. Z. (2008). A theoretical solution for pile-supported embankments on soft soils under one-dimensional compression. *Canadian Geotechnical Journal, 45*(5), 611–623.

Chew, S. H., Kamruzzaman, A. H. M., & Lee, F. H. (2004). Physico-chemical and engineering behavior of cement treated clays. *Journal of geotechnical and geoenvironmental engineering, 130*(7), 696–706.

Demir, A., Laman, M., Yildiz, A., & Ornek, M. (2013). Large scale field tests on geogrid-reinforced granular fill underlain by clay soil. *Geotextiles and Geomembranes, 38*, 1–15.

El Sawwaf, M. A. (2007). Behavior of strip footing on geogrid-reinforced sand over a soft clay slope. *Geotextiles and Geomembranes, 25*(1), 50–60.

Espinoza, R. D., & Bray, J. D. (1995). An integrated approach to evaluating single-layer reinforced soils. *Geosynthetics International, 2*(4), 723–739.

Fei, K., & Liu, H. L. (2009). Field test study and numerical analysis of a geogrid-reinforced and pile-supported embankment. *Rock and Soil Mechanics, 30*(4), 1004–1012, in Chinese.

Feng, W. Q., Li, C., Yin, J. H., Chen, J., & Liu, K. (2019). Physical model study on the clay–sand interface without and with geotextile separator. *Acta Geotechnica.* https://doi.org/10.1007/s11440-019-00763-4.

Hausmann, M. R. (1990). *Engineering principles of ground modification.* New York: The McGraw-Hill Companies Inc.

Ho, C. C. (2007). *The erosion behavior of revetment using geotextile* Doctoral dissertation. Université Joseph-Fourier-Grenoble I.

Kamruzzaman, A. H. M., Chew, S. H., & Lee, F. H. (2006). Microstructure of cement-treated Singapore marine clay. *Proceedings of the Institution of Civil Engineers - Ground Improvement, 10*(3), 113–123.

Kamruzzaman, A. H., Chew, S. H., & Lee, F. H. (2009). Structuration and destructuration behavior of cement-treated Singapore marine clay. *Journal of Geotechnical and Geoenvironmental Engineering, 135*(4), 573–589.

Kitazume, M., & Terashi, M. (2013). *The deep mixing method.* Boca Raton, USA: CRC Press.

Lai, H. J., Zheng, J. J., Zhang, R. J., & Cui, M. J. (2018). Classification and characteristics of soil arching structures in pile-supported embankments. *Computers and Geotechnics, 98*, 153–171.

Liu, G. S., Kong, L. W., Li, X. W., Ding, F., & Gu, J. (2008). Analysis of treatment scheme for soft foundation on in expressway widening project and its verification. *Chinese Journal of Rock Mechanics and Engineering, 27*(2), 309–315, in Chinese.

Low, B. K., Tang, S. K., & Choa, V. (1994). Arching in piled embankments. *Journal of Geotechnical Engineering, 120*(11), 1917–1938.

Rashid, A. S. A., Black, J. A., Kueh, A. B. H., & Noor, N. M. (2015). Behaviour of weak soils reinforced with soil cement columns formed by the deep mixing method: Rigid and flexible footings. *Measurement, 68*, 262–279.

Roy, S. S., & Deb, K. (2017). Bearing capacity of rectangular footings on multilayer geosynthetic sheet-reinforced granular fill over soft soil. *International Journal of Geomechanics, 17*(9), 04017069.

Russell, D., & Pierpoint, N. (1997). An assessment of design methods for piled embankments. *Ground Engineering, 30*(10), 39–44.

Sexton, B. G., Sivakumar, V., & McCabe, B. A. (2017). Creep improvement factors for vibro-replacement design. *Proceedings of the Institution of Civil Engineers - Ground Improvement, 170*(1), 35–56.

Shukla, S. K., & Yin, J. H. (2006). *Fundamentals of geosynthetic sheet engineering.* London, UK: Taylor & Francis Group.

van Eekelen, S. V., Bezuijen, A., & Van Tol, A. F. (2011). Analysis and modification of the British Standard BS8006 for the design of piled embankments. *Geotextiles and Geomembranes, 29*(3), 345–359.

Yin, J. H., & Fang, Z. (2006). Physical modelling of consolidation behaviour of a composite foundation consisting of a cement-mixed soil column and untreated soft marine clay. *Geotechnique, 56*(1), 63–68.

Yin, J. H., & Fang, Z. (2010). Physical modeling of a footing on soft soil ground with deep cement mixed soil columns under vertical loading. *Marine Georesources and Geotechnology, 28*(2), 173–188.

Yin, J. H., & Graham, J. (1994). Equivalent times and one-dimensional elastic viscoplastic modelling of time-dependent stress–strain behaviour of clays. *Canadian Geotechnical Journal, 31*(1), 42–52.

Yin, J. H., & Lai, C. K. (1998). Strength and stiffness of Hong Kong marine deposits mixed with cement. *Geotechnical Engineering, 29*(1), 29–43.

Zhang, J., Zheng, J. J., Chen, B. G., & Yin, J. H. (2013). Coupled mechanical and hydraulic modeling of a geosynthetic sheet-reinforced and pile-supported embankment. *Computers and Geotechnics, 52*, 28–37.

Zhuang, Y., Wang, K. Y., & Liu, H. L. (2014). A simplified model to analyze the reinforced piled embankments. *Geotextiles and Geomembranes, 42*(2), 154–165.

Further Reading

Bowles, J. E. (1996). *Foundation analysis and design* (5th ed.). New York: The McGraw-Hill Companies Inc.

Deb, K., Chandra, S., & Basudhar, P. K. (2007). Nonlinear analysis of multilayer extensible geosynthetic sheet-reinforced granular bed on soft soil. *Geotechnical and Geological Engineering, 25*(1), 11–23.

Labuz, J. F., & Theroux, B. (2005). Laboratory calibration of earth pressure cells. *Geotechnical Testing Journal, 28*(2), 188–196.